Multimeric connexin interactions prior to the trans-Golgi network

Jayasri Das Sarma[1], Rita A. Meyer[3], Fushan Wang[1], Valsamma Abraham[1], Cecilia W. Lo[2] and Michael Koval[1,*]

[1]University of Pennsylvania School of Medicine, Institute for Environmental Medicine and Department of Physiology and [2]Department of Biology, University of Pennsylvania, Philadelphia, PA 19104, USA and [3]Department of Biomedical Sciences, Creighton University, Omaha, NE 68178, USA
*Author for correspondence (e-mail: mkoval@mail.med.upenn.edu)

Accepted 7 August 2001
Journal of Cell Science 114, 4013-4024 (2001)

SUMMARY

Cells that express multiple connexins have the capacity to form heteromeric (mixed) gap junction hemichannels. We used a dominant negative connexin construct, consisting of bacterial β-galactosidase fused to the C terminus of connexin43 (Cx43/β-gal), to examine connexin compatibility in NIH 3T3 cells. Cx43/β-gal is retained in a perinuclear compartment and inhibits Cx43 transport to the cell surface. The intracellular connexin pool induced by Cx43/β-gal colocalized with a medial Golgi apparatus marker and was readily disassembled by treatment with brefeldin A. This was unexpected, since previous studies indicated that Cx43 assembly into hexameric hemichannels occurs in the trans-Golgi network (TGN) and is sensitive to brefeldin A. Further analysis by sucrose gradient fractionation showed that Cx43 and Cx43/β-gal were assembled into a subhexameric complex. Cx43/β-gal also specifically interacted with Cx46, but not Cx32, consistent with the ability of Cx43/β-gal to simultaneously inhibit multiple connexins. We confirmed that interactions between Cx43/β-gal and Cx46 reflect the ability of Cx43 and Cx46 to form heteromeric complexes, using HeLa and alveolar epithelial cells, which express both connexins. In contrast, ROS osteoblastic cells, which differentially sort Cx43 and Cx46, did not form Cx43/Cx46 heteromers. Thus, cells have the capacity to regulate whether or not compatible connexins intermix.

Key words: Gap junction, Hemichannel, Membrane traffic, Protein assembly, Heteromeric complex

INTRODUCTION

Gap junction channels are formed from transmembrane proteins known as connexins (Goodenough et al., 1996; Kumar and Gilula, 1996; Simon and Goodenough, 1998). Newly synthesized connexins (Cx) are first assembled into a hexameric hemichannel in an intracellular compartment, followed by transport to the plasma membrane (Yeager et al., 1998). Hemichannels at the plasma membrane then dock with hemichannels on adjacent cells to form a complete gap junction channel. Connexin assembly into gap junctions is also frequently accompanied by phosphorylation, which occurs predominantly, but not exclusively, at the cell surface (Cruciani and Mikalsen, 1999; Laird et al., 1995; Lampe et al., 1998; Musil et al., 1990).

While some key steps in connexin assembly have been outlined, the intracellular location of connexin assembly into hemichannels remains controversial, with evidence supporting both the endoplasmic reticulum (George et al., 1999; Kumar et al., 1995) and trans-Golgi network (TGN) (Koval et al., 1997; Musil and Goodenough, 1993) as assembly sites. This situation is complicated by the notion that different connexins may be assembled in different intracellular compartments (Yeager et al., 1998). Also, since a gap junction channel is composed of multiple subunits, cells that express more than one connexin have the capacity to form heteromeric (mixed) gap junction channels (Ahmad et al., 1999; Bevans et al., 1998; Brink et al., 1997; Jiang and Goodenough, 1996; Koval et al., 1995; Stauffer, 1995). Connexin structure is likely to be important in regulating heteromeric channel formation (Ahmad et al., 1999; Falk et al., 1997). However, it is also possible that cells use other mechanisms such as differential trafficking to regulate connexin interactions. For instance, we have found that a number of cell types which express both Cx43 and Cx46, including ROS cells (Koval et al., 1997) and alveolar epithelial cells (Abraham et al., 1999), show transport of Cx43 to the cell surface while Cx46 is retained in the trans-Golgi network. Whether this is due to differential sorting or incompatibility between Cx43 and Cx46 is not known at present.

Previous studies have shown that mutant connexins, either by design (Goliger et al., 1996; Krutovskikh et al., 1998; Paul et al., 1995; Sullivan and Lo, 1995) or through naturally occurring mutations (Kelsell et al., 2001), can have dominant negative effects on gap junctions. In some instances, dominant negative connexins have the capacity to interfere with connexin transport to the plasma membrane, which, in turn causes the retention of compatible connexins in intracellular compartments. Thus, the ability of a dominant negative connexin to interfere with the transport of another connexin may provide a method to rapidly screen for heteromeric connexin interactions. However, to date, the formation of a heteromeric complex between a dominant negative and native connexin has not been demonstrated. Here, we examined the trafficking of connexins in NIH-3T3 cells expressing a

dominant negative connexin, consisting of bacterial β-galactosidase (β-gal) fused to the C terminus of connexin43 (Cx43/β-gal). Earlier studies have shown that expression of Cx43/β-gal caused retention of native Cx43 in the perinuclear region of the cell (Sullivan and Lo, 1995). Using a combination of biochemical and morphological approaches, we determined the ability of Cx43/β-gal expressed by NIH-3T3 cells to specifically interact with three different connexins: Cx32, Cx43 and Cx46. We found that Cx43 and Cx46 formed heteromeric complexes with Cx43/β-gal and were retained in an intracellular compartment, while Cx32 was not. These results are consistent with the notion that a dominant negative connexin construct can specifically interfere with a subclass of connexins. Also, the interaction between Cx43/β-gal and Cx46 reflects the ability of unmodified Cx43 to interact with Cx46. However, by examining cells that show differential trafficking of Cx43 and Cx46, we found that cells control whether or not Cx43 and Cx46 intermix.

MATERIALS AND METHODS

Antisera and reagents

Rabbit anti-Cx43 (Civitelli et al., 1993) and anti-Cx46 (Koval et al., 1997) antisera were generated using a 6his-tagged C-terminal tail constructs as previously described. Rabbit anti-Cx32 was from Zymed (S. San Francisco, CA, USA). Polyclonal mouse anti-β-gal was from Sigma (St Louis, MO, USA) and polyclonal rabbit anti-β-gal was from Cappel (West Chester, PA, USA). Rhodamine-conjugated, FITC-conjugated and horseradish peroxidase-conjugated goat anti-rabbit IgG were from Roche Molecular Biochemicals (Indianapolis, IN, USA). Texas Red-conjugated goat anti-mouse IgG was from Jackson Immunoresearch (West Grove, PA, USA). BioMag magnetic particles coated with goat anti-mouse IgG were from Polysciences (Warrington, PA, USA). Triton X-100 was from Roche Molecular Biochemicals. Tissue culture reagents were from Life Technologies Inc/Gibco BRL (Rockville, MD, USA). Unless otherwise specified, all other reagents were from Sigma.

Cells

The stably transfected NIH 3T3 cells used in this study were previously generated by transfection of expression vectors that encoded for either β-galactosidase (β-gal) or a connexin43/β-galactosidase fusion protein (Cx43/β-gal) (Sullivan and Lo, 1995). Used in this study were stably transfected control clones expressing β-gal (E1A) or different levels of Cx43/β-gal (F2A and F4A, referred to here as 43β1 and 43β2, respectively). Stably transfected clones were selected with Dulbecco's modified Eagle medium (DMEM) + 10% fetal bovine serum containing 200 units hygromycin/ml and then divided into portions and frozen in 90% serum + 10% dimethyl sulphoxide (DMSO). Once thawed, the cells were used for no more than 20-25 passages. For some experiments, these same clones were also transiently transfected with either rat Cx46 (Koval et al., 1997) or rat Cx32 (Scherer et al., 1995) (kindly provided by Dr S. Scherer, University of Pennsylvania School of Medicine) using Lipofectamine (Life Technologies) and analyzed 48 hours after transfection. Primary rat alveolar epithelial cells were isolated and cultured as previously described (Abraham et al., 1999; Abraham et al., 2001) according to the method of Dobbs et al. (Dobbs et al., 1986) with modifications. ROS cells were cultured as previously described (Koval et al., 1997).

Protein preparation and analysis

Cells were washed, harvested into PBS containing protease inhibitors (10 mM N-ethyl maleimide, 1 mM phenylmethylsulfonyl chloride, 2 μg/ml leupeptin and 1 μg/ml pepstatin) and phosphatase inhibitors (1 mM $NaVO_4$ and 10 mM NaF) then passed through a ball-bearing homogenizer 100 times (Koval et al., 1997). The homogenate was centrifuged at 500 ***g*** for 5 minutes using an IEC CL3R centrifuge and then the resulting supernatant was centrifuged at 100,000 ***g*** for 30 minutes using a Beckman TL-100 ultracentrifuge to obtain a membrane-enriched pellet. To analyze total cell connexin expression, this pellet was resuspended in SDS-PAGE sample buffer.

For sucrose gradient fractionation, the membrane-enriched pellet was solubilized in 1% Triton X-100 and then overlayed onto a 5-20% sucrose gradient as previously described (Koval et al., 1997). In brief, the gradient was centrifuged at 148,000 ***g*** for 16 hours in a Sorvall Ultra Pro 80 centrifuge using a AH-650 swinging bucket rotor. Following centrifugation, 500 ml fractions were collected from the bottom of the centrifuge tube at 4°C, and then resolved by SDS-PAGE and Cx43 was detected by immunoblot analysis.

For detergent solubilization studies, the pellet was resuspended in PBS + inhibitors at 4°C containing 1% Triton X-100 and then incubated for 30 minutes at 4°C. Care was taken to insure that the samples were not warmed to room temperature during the extraction procedure. The sample was then centrifuged at 100,000 ***g*** for 30 minutes and separated into Triton X-100 soluble supernatant and insoluble pellet fractions (Koval et al., 1997; Musil and Goodenough, 1991). The soluble fraction was then diluted into 2× SDS-PAGE sample buffer, while the insoluble fraction was initially resuspended into PBS + 1% Triton X-100, prior to dilution.

For immunoblot, samples were resolved by SDS-PAGE using a 10% polyacrylamide gel, which was then transferred to PVDF membranes (transfer buffer: 50 mM Tris, 380 mM glycine, 0.025% SDS, 20% methanol). The samples were blocked overnight at room temperature (RT) using blotto (40 mM Tris, 5% (w:v) Carnation powdered milk and 0.1% (v:v) Tween-20), then incubated for 2 hours in primary antisera diluted in blotto, followed by a 1 hour incubation of horseradish peroxidase (HRP)-conjugated goat anti-rabbit IgG in blotto. The immunoblots were washed in PBS and then immunoreactive bands visualized using enhanced chemiluminescence (ECL, Amersham). Densitometric analysis of non-saturated films was performed using BioRad Quantity One analysis software (Hercules, CA, USA).

Immunopurification

Cells were homogenized and a Triton X-100 soluble fraction was isolated as described above. Magnetic goat anti-mouse IgG-coated particles were incubated for 2 hours with mouse anti-β-gal in PBS containing 0.25% BSA and 0.2% gelatin. The particles were then added to the Triton X-100 soluble fraction and incubated for 2 hours at 4°C. The magnetic particles were then isolated using a ceramic magnet (Stratagene, La Jolla, CA, USA). The particles were washed, resuspended in SDS-PAGE sample buffer and then analyzed by immunoblot.

Immunofluorescence

For standard immunofluorescence, cells plated on glass coverslips were fixed and permeabilized with methanol/acetone (1:1), then washed first with PBS, then PBS + 0.5% Triton X-100, then PBS + 0.5% Triton X-100 + 2% heat-inactivated goat serum (PBS/GS). The cells were incubated with primary antisera diluted into PBS/GS for 1 hour, washed, then labeled with secondary antisera diluted into PBS/GS. The cells were then washed with PBS, mounted into Mowiol and visualized by fluorescence microscopy using an Olympus IX-70 microscope system and imaged with a Hammatzu Orca-1 CCD camera and Image Pro image analysis software (Media Cybernetics, Silver Spring, MD, USA).

To preferentially label the TGN, we used a fluorescent lipid analogue, C_6-NBD-Cer (Pagano et al., 1989). Cells on glass coverslips were washed with PBS, fixed using 4% paraformaldehyde at RT for 10 minutes, washed with PBS, cooled to 4°C, then incubated with 5 pM C_6-NBD-Cer complexed to 0.34 mg/ml BSA. Excess C_6-NBD-

Cer was then removed by back exchange using 4× 10 minute washes at 4°C with PBS containing 3.4 mg/ml defatted BSA, and the cells were washed in PBS. The coverslips were then mounted in a microscope stage chamber (Harvard Apparatus, South Natick, MA, USA), covered with PBS and imaged by fluorescence microscopy.

For in situ Triton X-100 extraction (Musil and Goodenough, 1991; Musil and Goodenough, 1993), cells were first cultured on poly-D-lysine/laminin coverslips (Becton Dickinson, Bedford, MA, USA) for 2 days. The cells were then incubated in PBS containing 0.675 mM $CaCl_2$, 0.2 mM $MgCl_2$ and 1% Triton X-100 for 30 minutes at 15°C, washed with PBS, fixed with methanol/acetone and analyzed by immunofluorescence microscopy as described above.

Immunogold electron microscopy

For postembedding immunogold electron microscopy (EM), cells were first washed four times with PBS, fixed with 2.5% glutaraldehyde in PBS for 30 minutes at RT, washed four times with PBS, treated with 1% OsO_4 in 0.1 M phosphate buffer for 1 hour, then washed four times with H_2O. The samples were dehydrated using increasing concentrations of acetone in H_2O, then embedded in Embed 812/Araldite, which was hardened at 55°C overnight. Thin sections were immunolabeled with mouse anti-Cx43 (Chemicon) and rabbit anti β-gal (Cappel) diluted in PBS/GS, washed and then labeled with secondary antisera diluted into PBS/GS 15 nm anti-mouse IgG and 5 nm anti-rabbit IgG (AuroProbe EM, Amersham). Sections were imaged using a Hitachi transmission electron microscope.

RESULTS

Cx43/β-gal disrupts Cx43 transport to the plasma membrane

We examined Cx43 trafficking in two NIH-3T3 fibroblast cell lines, 43β1 and 43β2, which were stably transfected to express a Cx43 fusion protein construct containing bacterial β-galactosidase (β-gal) attached to the C terminus (Cx43/β-gal) (Sullivan and Lo, 1995). These cells were compared to control NIH-3T3 cells stably transfected with β-gal alone (con). As shown by immunoblot (Fig. 1), all three cell lines express endogenous Cx43 as a series of bands ranging from 42-46 kDa, depending upon phosphorylated state (Musil et al., 1990; Musil and Goodenough, 1991). Cx43/β-gal is simultaneously recognized by anti-Cx43 antiserum predominantly as a 160 kDa species, which enabled us to calculate the ratio of Cx43/β-gal expression to endogenous Cx43. Using this approach, we estimate that 43β2 cells expressed 5.3-fold (±0.3; n=3) more Cx43/β-gal than 43β1 cells. 43β1 cells expressed roughly one Cx43/β-gal for every 8.4±3.1 (n=3) molecules of endogenous Cx43, while 43β2 cells expressed one Cx43/β-gal for every 1.5±0.6 (n=3) Cx43 molecules (Fig. 1B). The relative level of Cx43/β-gal expressed by these cells correlated with the extent of inhibition for gap junctional communication as previously described (Sullivan and Lo, 1995).

Previous studies have shown that Cx43 phosphorylation to the 44 and 46 kDa isoforms occurs after delivery to the cell surface (Cruciani and Mikalsen, 1999; Laird et al., 1995; Lampe et al., 1998; Musil et al., 1990). The relative amount of the 42 kDa isoform of Cx43 was higher for 43β1 and 43β2 cells than control cells (Fig. 1C), which suggested that increasing levels of Cx43/β-gal expression caused increased Cx43 retention in an intracellular compartment. This was confirmed by immunofluorescence microscopy. Consistent with previous results (Sullivan and Lo, 1995), we observed an

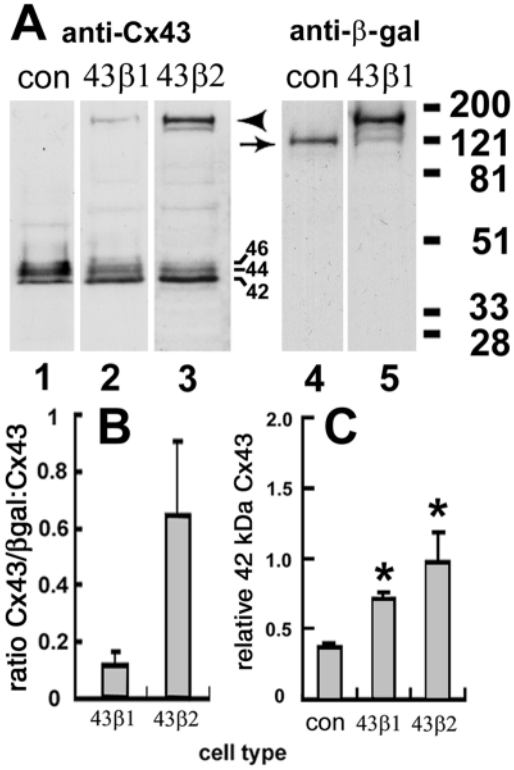

Fig. 1. Cx43/β-gal expression increased endogenous Cx43 expression. (A) Membrane-enriched fractions prepared from cells stably transfected with either β-gal (con, lanes 1, 4) or Cx43/β-gal (43β1, lanes 2, 5; 43β2, lane 3) were resolved by SDS-PAGE, transferred to PVDF and then immunoblotted using rabbit antisera to either Cx43 (lanes 1-3) or to β-gal (4-5) and detected with enhanced chemiluminescence. The arrowhead indicates the band representing the Cx43/β-gal fusion protein, while the arrow indicates β-gal. The lower molecular mass band appearing in some samples of Cx43/β-gal is a truncation product, as previously described (Sullivan and Lo, 1995). The 44 and 46 kDa Cx43 isoforms correspond to phosphorylated Cx43. Note the increase in amount of the faster migrating 42 kDa Cx43 isoform in cells expressing Cx43/β-gal. The positions of molecular markers (kDa) are shown. (B) Immunoblots from 43β1 and 43β2 cells were quantified by densitometry to obtain the amount of Cx43/β-gal expression relative to endogenous Cx43. Cx43/β-gal expression by 43β2 cells was five- to sixfold higher than for 43β1 cells. (C) Immunoblots from control, 43β1 and 43β2 cells were quantified for the amount of the 42 kDa Cx43 isoform, normalized to the total level of Cx43 expressed by control cells. Values are means ± s.e.m. of triplicate preparations. *Statistically significant from control (P<0.05).

increase in intracellular Cx43 immunoreactivity and a decrease in cell surface Cx43 immunoreactivity for 43β1 and 43β2 cells (Fig. 2). Also, 43β2 cells had more intracellular Cx43/β-gal than 43β1 cells, consistent with the total amount of Cx43/β-gal expressed by these cells.

Intracellular Cx43/β-gal is in a Triton X-100 soluble pool

To further investigate the intracellular distribution of Cx43, 43β1 and 43β2 cells were examined after Triton X-100 extraction. Musil and Goodenough (Musil and Goodenough, 1991) have shown that Cx43 assembled into gap junction plaques is resistant to Triton X-100 solubilization at 4°C, while

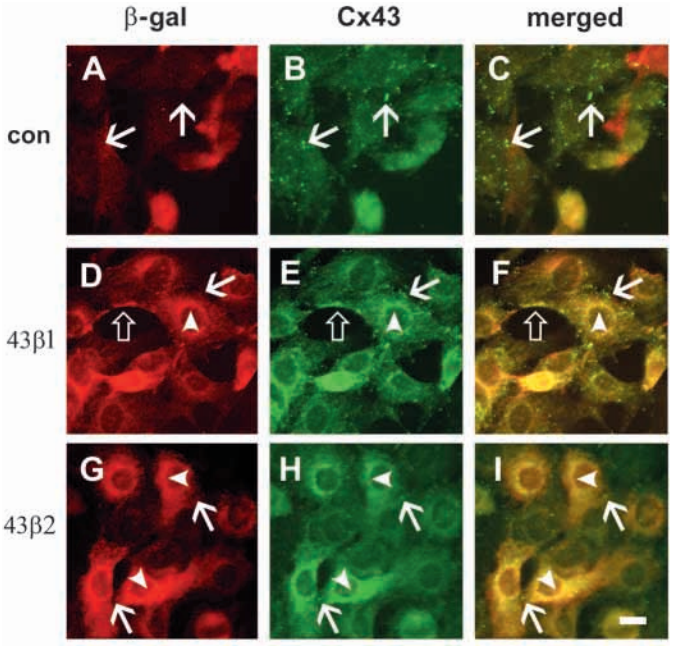

Fig. 2. Cx43/β-gal expression alters the intracellular distribution of endogenous Cx43. Control (A-C), 43β1 (D-F) and 43β2 (G-I) cells were fixed, permeabilized and then double-label immunostained using mouse anti-β-gal (A,D,G) and rabbit anti-Cx43 (B,E,H), detected using Texas Red-conjugated goat anti-mouse IgG and FITC-conjugated goat anti-rabbit IgG as secondary antibodies. With increasing Cx43/β-gal expression, there was increased perinuclear localization of both the anti-β-gal and anti-Cx43 signals (arrowheads). Also, while control cells had numerous areas showing labeling by Cx43 alone in areas where cells are in close apposition (arrows), this was less apparent for cells expressing high levels of Cx43/β-gal. Note the plasma membrane regions of 43β1 cells, which showed labeling by both anti-β-gal and anti-Cx43 (open arrows). Bar, 10 μm.

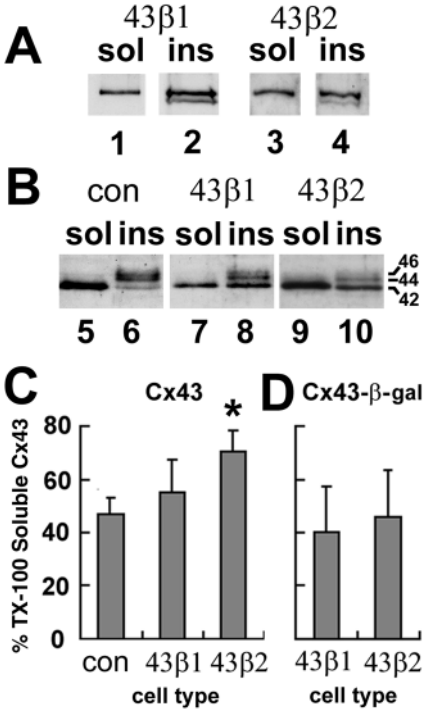

Fig. 3. Triton X-100 extraction of Cx43/β-gal and Cx43. Membrane preparations obtained from control (con) or Cx43/β-gal transfected cells (43β1, 43β2) were incubated in Triton X-100 at 4°C for 30 minutes and then centrifuged at 100,000 ***g*** for 30 minutes to separate Triton X-100 soluble (sol) and insoluble (ins) fractions. The soluble and insoluble fractions were then resolved by electrophoresis, and detected by immunoblot for Cx43/β-gal (A) and Cx43 (B). Cx43 samples that had the best resolution of the three Cx43 isoforms are shown. The amount of Triton X-100 soluble Cx43 (C) and Cx43/β-gal (D) was determined by densitometry. The amount of Cx43 in the Triton X-100 soluble fraction was significantly higher for 43β2 cells, consistent with decreased incorporation into gap junction plaques. *Statistically significant from control (P<0.05).

Cx43 not assembled into gap junctions remains Triton X-100 soluble. Thus, compared to control cells, the relative amount of Triton X-100 soluble Cx43 should increase for 43β1 and 43β2 cells, where there was an increase in intracellular Cx43. As shown in Fig. 3C, this was the trend, with a significantly higher level of Cx43 in the Triton X-100 soluble pool for 43β2 cells.

Interestingly, the Triton X-100 insoluble fraction isolated from 43β1 and 43β2 cells was enriched for the 42 kDa isoform of Cx43, as opposed to control cells (Fig. 3B). The ratio of the 42 kDa Cx43 isoform to the higher molecular mass Cx43 isoforms was 0.57±0.24 (n=3) for control cells, while 43β2 cells had a ratio of 1.20±0.11 (n=3), reflecting a twofold enrichment of the 42 kDa isoform in the Triton X-100 insoluble pool. Given that Cx43 phosphorylation to the 44 and 46 kDa isoforms occurs predominantly at the cell surface (Cruciani and Mikalsen, 1999; Laird et al., 1995; Lampe et al., 1998; Musil et al., 1990), this raised the possibility that the intracellular Cx43 pool may be due to a Triton X-100 insoluble complex with Cx43/β-gal. However, since approximately 40% of the Cx43/β-gal expressed by 43β1 and 43β2 cells was Triton X-100 soluble (Fig. 3D), formation of an insoluble intracellular complex did not seem likely.

To directly determine the localization of the Triton X-100 soluble and insoluble Cx43/β-gal fractions, we performed in situ Triton X-100 extraction (Musil and Goodenough, 1991). Triton X-100 extracted control cells showed substantial Cx43 localized to the plasma membrane (Fig. 4E,F). In contrast, most of the intracellular pool of Cx43/β-gal was readily extracted by Triton X-100, although there was also some Triton X-100 resistant Cx43/β-gal localized to the plasma membrane in 43β2 cells (Fig. 4). Note that the immunofluorescence images of Triton X-100 extracted cells were obtained at higher gain settings than unextracted cells (see Fig. 4, legend). Thus, images of Triton X-100 extracted cells obtained at a comparable gain to controls would have appeared faint, consistent with the paucity of Cx43 and Cx43/β-gal labeling observed in unextracted cells (see also Fig. 2). Note that approx. 5-10% of the 43β2 cells detached during Triton X-100 extraction, leaving areas of Cx43 localization which appeared not to be in contact with other cells. Also, there were occasional cells that contained some Triton X-100 resistant Cx43/β-gal with an intracellular localization, possibly due to premature formation of an intracellular Triton X-100 insoluble complex or perhaps localizing to an aggresome as a result of overexpression (Garcia-Mata et al., 1999; Johnston et al., 1998). Nonetheless, considering the gain settings for the

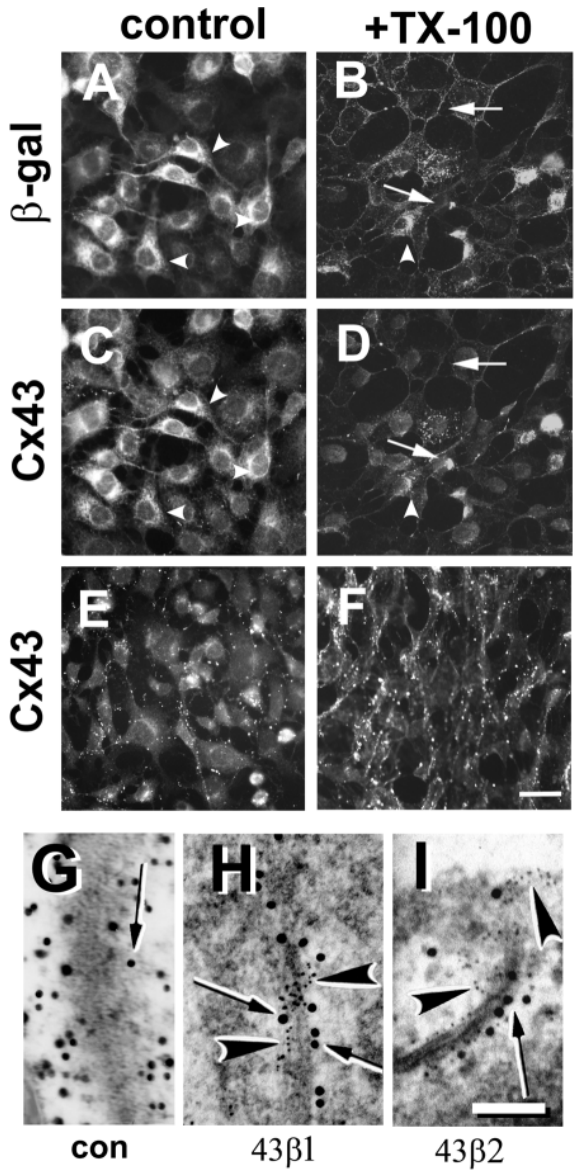

Fig. 4. Intracellular Cx43/β-gal is Triton X-100 soluble. 43β2 cells (A-D) or control cells (E,F) were incubated with PBS alone (A,C,E) or PBS containing 1% Triton X-100 (B,D,F) for 30 minutes at 15°C, then washed, fixed and immunostained using mouse anti-β-gal antisera (A,B) and rabbit anti-Cx43 (C,D) or rabbit anti-Cx43 alone (E,F). The cells were then stained with FITC-conjugated goat anti-rabbit IgG and Texas Red-conjugated goat anti-mouse IgG. β-gal images were obtained at 350 millisecond exposure with gain settings of 15 for unextracted cells (A) and 100 for Triton X-100 extracted cells (B), while Cx43 images were obtained at 1.5 second exposure with gain settings of 70 (C,E) and 200 (D,F). Triton X-100 extracted nearly all intracellular Cx43/β-gal (arrowheads), revealing the Triton X-100 resistant pool of Cx43/β-gal at the plasma membrane (arrows). Note the relatively higher Cx43 immunofluorescence signal from Triton X-100 extracted control cells (F), as compared to 43β2 cells (D). Bar, 30 μm. (G-I) Control (G), 43β1 (H) and 43β2 (I) cells were processed for EM immunogold labeling as described in Materials and Methods and labeled using mouse anti-Cx43/15 nm gold-conjugated goat anti mouse IgG (arrows) and rabbit anti-β-gal/5 nm gold-conjugated goat anti-rabbit IgG (arrowheads). Labeling for both Cx43 and Cx43/β-gal was present in 43β1 and 43β2 cells (H,I), but not control cells (G). Bar, 100 nm.

images obtained for Triton X-100 extracted cells, this intracellular pool is small compared to the intracellular pool for unextracted cells. Similar results were obtained for in situ extraction of 43β1 cells (not shown).

Since Triton X-100 extraction revealed some Cx43/β-gal at the plasma membrane of 43β2 cells, we used postembedding immunogold EM analysis to determine whether this was localized to gap junction plaques. As shown in Fig. 4G-I, β-gal transfected control cells showed Cx43 immunolabeling, but not β-gal labeling (representative of eight gap junction profiles). Results from non-transfected 3T3 cells were similar to controls (10 profiles; not shown). However, both 43β1 and 43β2 cells showed immunogold labeling corresponding to both Cx43 and β-gal localized to gap junction plaques. While gap junctions visible by EM were rare, the data shown in Fig. 5B,C are representative images from 6 and 10 gap junction profiles, from 43β1 and 43β2 cells, respectively. Thus, combined with our immunofluorescence analysis of Triton X-100 extracted cells, our data are consistent with the idea that there is some Cx43/β-gal assembled into gap junctions.

Also, consistent with an effect of Cx43/β-gal on gap junction plaque assembly by Cx43/β-gal, we observed that the gap junctions associated with 43β1 and 43β2 cells were smaller than plaques from control cells or 43β1 cells. The average length of gap junctions for control cells was 486±44 nm (n=8), while average gap junction length for 43β1 and 43β2 cells was 246±31 nm (n=6) and 226±23 nm (n=10), respectively. Thus, the decreased gap junctional communication between cells expressing Cx43/β-gal (Sullivan and Lo, 1995) may be due in part to the smaller gap junction contacts between the cells.

Cx43 and Cx43/β-gal form a Triton X-100 stable complex in an early secretory compartment

To further define the subcellular localization of Cx43/β-gal, we used antibody MG160 as a marker for the Golgi region of the cell (Gonatas et al., 1989). As shown in Fig. 5A,B, the perinuclear staining pattern for β-gal colocalized with MG160, consistent with Cx43/β-gal accumulation in one or more aspects of the Golgi apparatus. When 43β2 cells were incubated with brefeldin A (BFA) for 5 minutes prior to immunolabeling to stimulate the disassembly of the cis and medial Golgi apparatus stacks into the ER (Lippincott-Schwartz et al., 1989), the bright perinuclear fluorescence disappeared, indicating that both Cx43/β-gal and MG160 relocalized to the ER (Fig. 5E,F). Note that 43β2 cells treated with BFA and double-labeled with anti-Cx43 and anti-β-gal showed coincident ER localization for both antisera (data not shown).

43β2 cells treated with BFA for 30 minutes also showed Cx43/β-gal localized to the ER (Fig. 5H), rather than the region of the centriole, which would be characteristic for a TGN-localized protein (Koval et al., 1997; Lippincott-Schwartz et al., 1991; Reaves and Banting, 1992). To confirm that a 30 minute treatment of NIH 3T3 cells with BFA caused the TGN to condense in the region of the centriole, we used C_6-NBD-Cer to preferentially label the TGN (Fig. 5C). As shown in Fig. 5G, C_6-NBD-Cer labeled a cluster of vesicles in the pericentriolar region of 43β2 cells treated with BFA for 30 minutes, characteristic of the effect of BFA on the TGN and in contrast to the localization pattern for Cx43/β-gal in comparably treated 43β2 cells (Fig. 5H). In particular, a 30

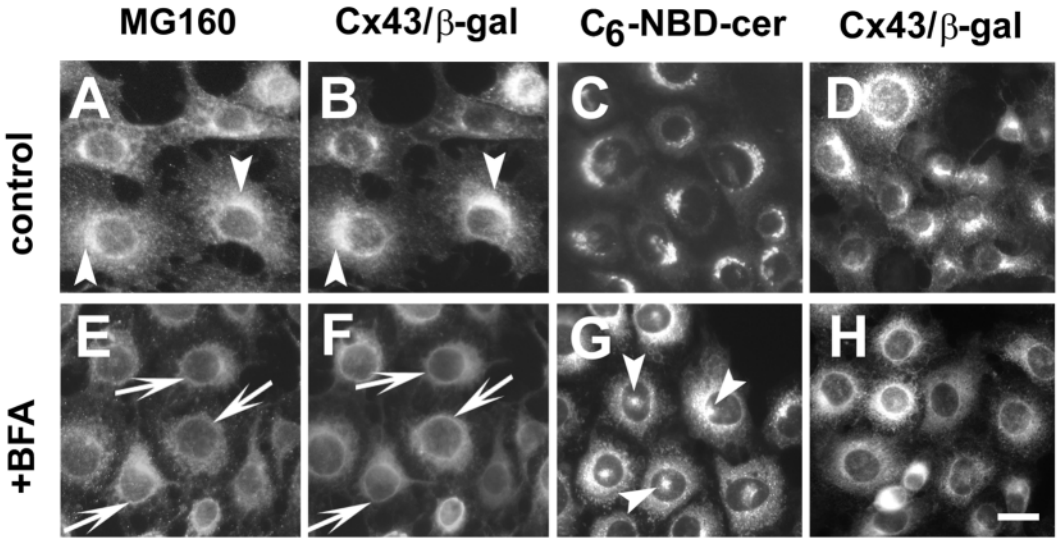

Fig. 5. Intracellular Cx43/β-gal is in an early secretory compartment. 43β2 cells were incubated in either the absence (A-D) or presence (E-H) of 5 μg/ml brefeldin A (BFA) for either 5 minutes (E,F) or 30 minutes (G,H) to collapse the cis and medial aspects of the Golgi apparatus into the ER. (A,B,E,F) The cells were then fixed, permeabilized and double-label immunostained using mouse anti-MG160 (A,E) and rabbit anti-β-gal (B,F), which were detected using Texas Red-conjugated goat anti-mouse IgG and FITC-conjugated goat anti-rabbit IgG as secondary antibodies, respectively. Arrowheads indicate perinuclear regions where there was good colocalization between MG160 and Cx43/β-gal (A,B). Note that both MG160 and Cx43/β-gal were translocated to the ER by BFA treatment, as revealed by an increase in nuclear membrane (E,F, arrows) and peripheral labeling. (C,G) 43β2 cells (C) treated to preferentially label the TGN with C_6-NBD-Cer (as described in Materials and Methods) showed perinuclear labeling, while 43β2 cells pretreated with BFA for 30 minutes (G) showed a characteristic TGN labeling pattern (arrowheads). (D,H) In a parallel set of cells, treatment for 30 minutes with BFA (H) did not cause Cx43/β-gal to accumulate in a condensed TGN structure. Bar, 20 μm.

minute treatment of cells with BFA did not induce a pericentriolar cluster of vesicles containing Cx43/β-gal. Taken together, these results suggest that most of the intracellular Cx43/β-gal pool was localized to compartments prior to the TGN in 43β2 cells.

Our finding that the intracellular pool of Cx43/β-gal was sensitive to BFA was surprising, since Cx43/β-gal interfered with Cx43 transport and the TGN has been implicated as the site for Cx43 assembly in other cell types (Koval et al., 1997; Musil and Goodenough, 1993). As a direct measure to determine whether there was a heteromeric interaction between these two connexins, we examined whether endogenous Cx43 coimmunopurified with Cx43/β-gal, using anti-β-gal antiserum. Triton X-100 soluble extracts prepared at 4°C were used, since Cx43 oligomers are stable under these conditions and this eliminates connexins assembled into gap junction plaques and higher order connexin aggregates that might complicate the analysis (Koval et al., 1997; Musil and Goodenough, 1993).

As shown in Fig. 6A, endogenous Cx43 and Cx43/β-gal coimmunopurified from Triton X-100 solubilized extracts using anti-β-gal antiserum, consistent with the formation of a mixed Cx43-Cx43/β-gal complex by 43β1 and Cx43β2 cells. Note that only the 42 kDa Cx43 isoform of endogenous Cx43 was detected, since higher molecular mass Cx43 isoforms were not soluble in Triton X-100 at 4°C (see Fig. 3B). Also, endogenous Cx43 was not immunopurified using anti-β-gal antiserum from control cells expressing β-gal alone, indicating that there was little, if any, non-specific absorption of Cx43 to the magnetic particles.

Given the interaction of Cx43 with Cx43/β-gal in a compartment prior to the TGN, we used sucrose gradient fractionation analysis of control and 43β2 cells solubilized in Triton X-100 to determine the oligomeric state of Cx43 and Cx43/β-gal complexes (Fig. 6B,C). In control cells, 14.8±4.6% (n=3) of the Triton X-100 soluble Cx43 was assembled into heximeric complexes (region 3 of the gradient). Treatment of control cells with BFA for 30 minutes reduced the level of Cx43 assembly to 2.7±3.8% (n=2) of the Triton X-100 soluble pool, consistent with previous results for other cell types (Musil and Goodenough, 1993).

For sucrose gradients prepared from 43β2 cells, the Triton X-100 soluble fraction of Cx43/β-gal appeared as a heavy fraction at the bottom of the gradient and as a peak of intermediate molecular mass (gradient region 2), as compared to the monomer (region 1) and hemichannel Cx43 peaks (region 3) observed for control cells. There was not any detectable Cx43/β-gal in the 25% sucrose cushion at the bottom of the centrifuge tube. In these gradients from 43β2 cells, there was also a peak of endogenous Cx43, which coincided with the Cx43/β-gal peak (gradient region 2), while less than 2% of the endogenous Cx43 coincided with the heavy Cx43/β-gal fraction (region 4). The intermediate Cx43 peak is most likely due to the interaction between Cx43 and Cx43/β-gal, since Cx43 and Cx43/β-gal formed a coimmunoisolatable complex (Fig. 6A). Of the total Triton X-100 soluble Cx43 isolated from 43β2 cells, 11.9±3.8% (n=2) was in the fractions that also contained Cx43/β-gal. In contrast, gradient region 2 for control cells contained only 4.4±2.0% (n=3) of the total Triton X-100 soluble Cx43. Also, the amount of Cx43 in the hexamer peak (region 3) was reduced to 6.7±0.1% (n=2) by expression of Cx43/β-gal as compared to 14.8% for control

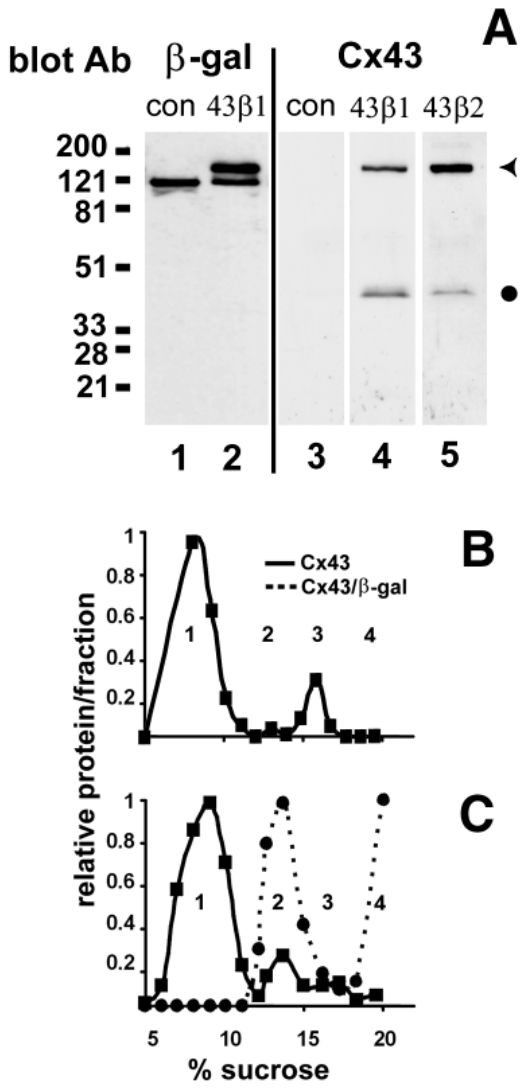

Fig. 6. Direct interaction between endogenous Cx43 with Cx43/β-gal. (A) Membrane preparations from control (lanes 1, 3), 43β1 (lanes 2, 4) and 43β2 cells (lane 5) were solubilized in 1% Triton X-100 at 4°C for 30 minutes and then centrifuged at 100,000 ***g*** for 30 minutes to remove insoluble material. The supernatant was then incubated with mouse anti-β-gal antiserum and goat anti-mouse IgG-conjugated magnetic beads, then magnetically isolated and solubilized in SDS-PAGE sample buffer. The resulting samples were resolved by electrophoresis, immunoblotted using rabbit antisera which recognizes either β-gal (lanes 1, 2) or Cx43 (lanes 3-5), then detected by chemiluminescence. The arrowhead indicates bands corresponding to Cx43/β-gal, while the dot indicates endogenous Cx43. (B,C) Membrane-enriched fractions from control cells (B) or 43β2 cells (C) were solubilized in Triton X-100 and then analyzed by sucrose gradient fractionation as described in Materials and Methods. The solid line indicates fractions containing unmodified, endogenous Cx43 while the broken line in C corresponds to Cx43/β-gal. Region 1 of the gradient (5%-11% sucrose) corresponds to Cx43 monomers, while Cx43 hexamers sediment at region 3 of the gradient (approx. 15%-18% sucrose), peaks that correspond to 5S (HRP) and 9S (catalase) standards, respectively. Expression of Cx43/β-gal caused an increase in Cx43 which cosedimented in region 2 of the gradient (11%-15% sucrose). Region 4 of the gradient (18%-20% sucrose) from 43β2 cells contained some Cx43/β-gal complexes, but showed little, if any native Cx43.

cells. Thus, Cx43/β-gal both disrupted the formation of Cx43-containing hemichannels and caused the appearance of a heteromeric complex in 43β2 cells of intermediate molecular mass.

The molecular mass of the intermediate complex in region 2 was between that of monomeric Cx43 (approx. 43 kDa) and hexameric Cx43 hemichannels (approx. 258 kDa). Based on estimates of molecular mass, the intermediate peak is likely to correspond to a Cx43 + Cx43/β-gal heterodimer (approx. 43 kDa+159 kDa=approx. 202 kDa). However, the resolution of our sucrose gradients was not sufficient to rule out a potential heteromeric complex between Cx43, Cx43/β-gal and other, as yet unidentified, proteins. Most, if not all, of the Cx43 that coimmunoisolated with Cx43/β-gal was likely to be assembled into these intermediate complexes, since there was little Cx43 which comigrated with Cx43/β-gal assembled into the higher molecular mass complex.

Interactions between Cx43/β-gal and other connexins

To determine whether Cx43/β-gal had the potential to interact with connexins in addition to Cx43, we transiently transfected Cx32 or Cx46 into either control, 43β1 or 43β2 cells. As shown by immunofluorescence microscopy (Fig. 7), Cx32 showed little overlap with Cx43/β-gal, suggesting that Cx32 trafficking was independent of Cx43/β-gal. In contrast, Cx46 and Cx43/β-gal showed good colocalization, particularly in the perinuclear region of the cell (Fig. 8). Also, transiently transfected 43β1 and 43β2 cells showed decreased Cx46 at the cell surface, consistent with the notion that Cx46

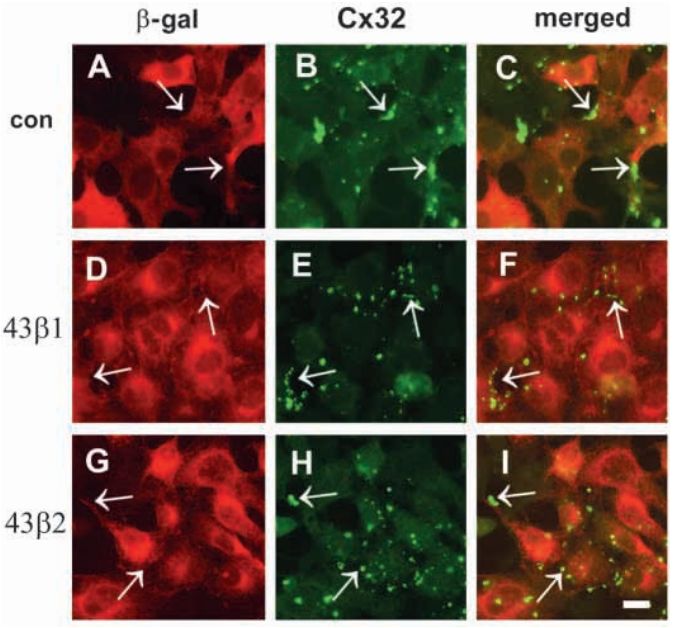

Fig. 7. Cx32 does not colocalize with Cx43/β-gal. Control (con; A-C), 43β1 (D-F) and 43β2 (G-I) cells were transiently transfected with Cx32 and allowed to recover for 48 hours. The cells were fixed, permeabilized and then double-label immunostained using mouse anti-β-gal (A,D,G) and rabbit anti-Cx32 (B,E,H) antisera, which were detected using Texas Red-conjugated goat anti-mouse IgG and FITC-conjugated goat anti-rabbit IgG as secondary antibodies, respectively. The intracellular distribution of Cx32 was not affected by Cx43/β-gal expression (arrows). Bar, 10 μm.

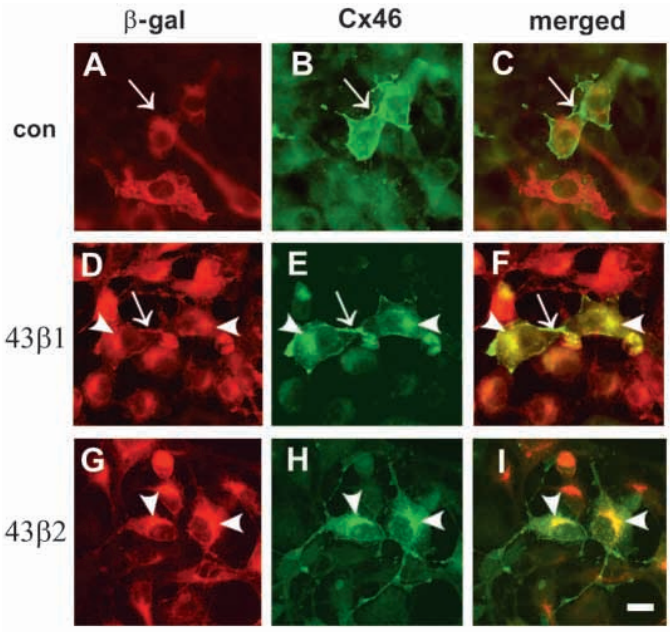

Fig. 8. Cx46 transport is inhibited by Cx43/β-gal. Control (con; A-C), 43β1 (D-F) and 43β2 (G-I) cells were transiently transfected with Cx46 and allowed to recover for 48 hours. The cells were fixed, permeabilized and then double-label immunostained using mouse anti-β-gal (A,D,G) and rabbit anti-Cx46 (B,E,H) antisera, which were detected using Texas Red-conjugated goat anti-mouse IgG and FITC-conjugated goat anti-rabbit IgG as secondary antibodies, respectively. Cells showed colocalization of Cx43/β-gal with both Cx46 at the cell surface (arrows) and Cx46 retained in the perinuclear region of the cell (arrowheads). Note the increased retention of Cx46 by 43β2 cells, as compared to 43β1 cells. Bar, 10 μm.

transport to the cell surface was inhibited by Cx43/β-gal expression (Fig. 8).

To confirm that the effect of Cx43/β-gal on Cx46 trafficking correlated with the ability of Cx43/β-gal to form a heteromeric complex with Cx46, coimmunopurification experiments were done using transiently transfected cells. As shown in Fig. 9A, Cx46 coimmunopurified from Triton X-100 solubilized 43β1 cells using anti-β-gal antiserum. We did observe some non-specific immunoisolation of Cx46 (lane 11), but this was only 5.8±2.7 (n=3)% of the specific signal (lane 12). Interestingly, the Cx46 immunoisolated with Cx43/β-gal was enriched for the 53 kDa, non-phosphorylated isoform (Jiang et al., 1993; Konig and Zampighi, 1995), which would be expected if these two proteins interacted in an intracellular compartment (Koval et al., 1997). Thus, Cx43/β-gal had the capacity to form specific heteromeric complexes with Cx46 in addition to Cx43. In contrast, Cx32 was not coimmunopurified using anti-β-gal antiserum from either control or 43β1 cells transfected with Cx32. This further confirms that the interaction between Cx43/β-gal and either Cx43 or Cx46 was specific.

Recently, Berthoud et al. showed that Cx43 can oligomerize with Cx56, the chick ortholog of Cx46 (Berthoud et al., 2000). Given this and the observation that Cx46 coimmunoisolated with Cx43/β-gal, we wanted to determine whether Cx46 would also oligomerize with unmodified Cx43 expressed in cells. Hela or Hela/Cx43 cells were transiently transfected with Cx46 and the ability of Cx46 to be specifically immunoisolated using anti-Cx43 was determined (Fig. 9, lanes 13-18). Consistent with results obtained with Cx43/β-gal, Cx43 and Cx46 formed immunoisolatable oligomers, enriched for the 53 kDa Cx46 isoform (lane 18), while cells expressing Cx46 alone showed little, if any, Cx46 immunopurified using anti-Cx43 IgG (lane 17).

We also examined the ability of Cx43 and Cx46 to interact in cells that produce both proteins endogenously and that show differential trafficking of these two proteins. Primary rat alveolar epithelial cells, cultured to differentiate to a type I-like phenotype, transport both Cx43 and Cx46 to the plasma membrane (Abraham et al., 1999; Abraham et al., 2001) (Fig. 9G-I). In contrast, ROS osteoblastic cells transport Cx43 to the plasma membrane, but retain Cx46 in the TGN (Koval et al., 1997) (Fig. 9D-F). As shown in Fig. 9, lane 22, Cx46 was specifically immunopurified from alveolar epithelial cell extracts using anti-Cx43 IgG, consistent with formation of heteromeric Cx43/Cx46 gap junctions by these cells. However, Cx46 was not immunoisolatable from ROS cells using anti-Cx43 IgG (Fig. 9, lane 21). Thus, despite the ability of Cx43 and Cx46 to form heteromeric gap junctions in other cell systems, our data suggest that ROS cells possess a mechanism for preventing Cx43 and Cx46 from heteromeric oligomerization.

DISCUSSION

Regulation of heteromeric interactions between Cx43 and Cx46

We found that Cx43/β-gal forms specific heteromeric complexes with Cx43 and Cx46, but not with Cx32. This is also the case with cells expressing unmodified Cx43 and Cx46 (Fig. 9). This demonstration from intact cells that Cx43 and Cx46 have the capacity to interact is consistent with the observations of Berthoud et al. (Berthoud et al., 2000), who found that Cx56, the chick ortholog of Cx46, and Cx43 formed heteromeric channels.

However, as shown in Fig. 9, Cx46 expressed by ROS cells did not coimmunopurify with Cx43. This is a key point, since this demonstrated that the ability of cells to form heteromeric connexins is not a function of random intermixing of compatible connexins but depends on the context of expression, since ROS cells show differential trafficking of Cx43 and Cx46, where Cx46 alone is retained in the TGN. We have also found that Cx43 and Cx46 show differential trafficking in alveolar epithelial cells, depending on cell phenotype (Abraham et al., 1999). As demonstrated here, alveolar epithelial cells with a type I phenotype transported Cx43 and Cx46 to the plasma membrane and assembled them into heteromeric complexes. However, the intracellular distribution of Cx43 and Cx46 expressed by type II alveolar epithelial cells is comparable to ROS cells, where Cx43 is at the plasma membrane and Cx46 is retained in the TGN (Abraham et al., 1999). Since Cx46 is dramatically upregulated by alveolar epithelial cells in response to oxidant-mediated lung injury in vivo (Abraham et al., 2001), alveolar epithelial cells are likely to use regulation at the level of both transcription and trafficking to control the formation of Cx43/Cx46 heteromeric gap junction channels. The function of these heteromeric channels in lung injury is not known at

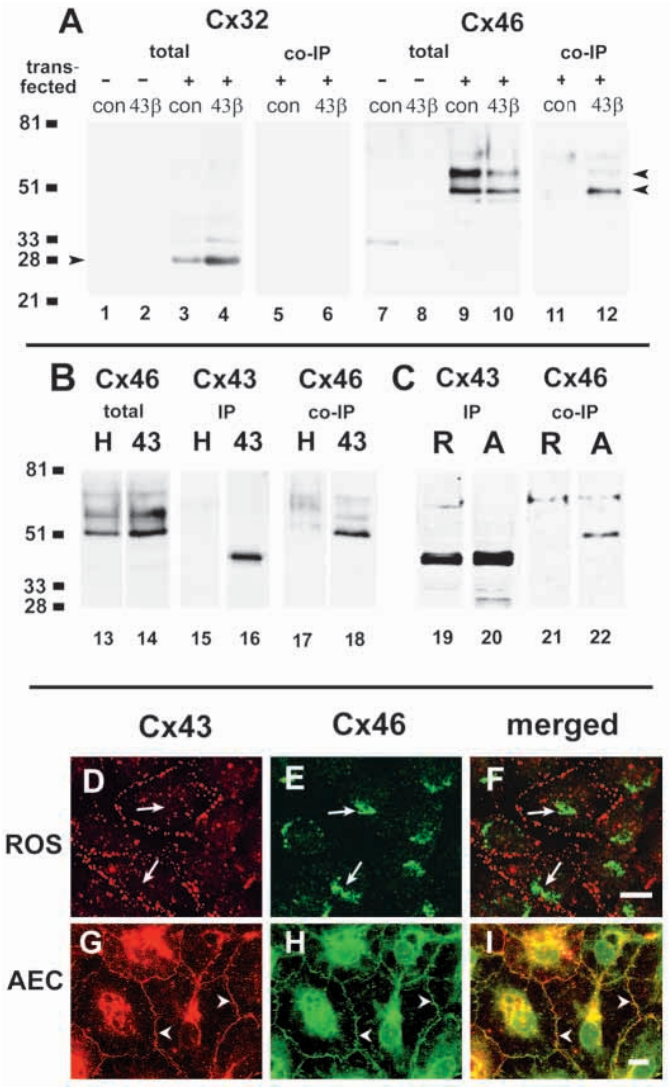

Fig. 9. Cx43 and Cx43/β-gal specifically interact with Cx46. (A) Membrane preparations from either non-transfected cells (lanes 1, 2, 7, 8) or cells transiently transfected with either Cx32 (lanes 3-6) or Cx46 cDNA (lanes 9-12) were Triton X-100 solubilized and immunopurified using mouse anti-β-gal as described in Fig. 6. The resulting samples were resolved by electrophoresis, immunoblotted using rabbit antisera that recognizes either Cx32 (lanes 1-6) or Cx46 (lanes 7-12), then detected by chemiluminescence. Arrowheads denote bands corresponding to Cx32 (approx. 28 kDa), phosphorylated Cx46 (approx. 68 kDa) and nonphosphorylated Cx46 (approx. 53 kDa). Occasionally, the anti-Cx46 antibody recognized a non-specific band of apparent molecular mass approx. 75 kDa. Cx46, but not Cx32, was immunopurified using anti-β-gal antiserum (lane 12), suggesting that Cx43/β-gal and Cx46 formed a specific oligomeric complex. (B) To confirm the ability of unmodified Cx43 to coimmunoprecipitate with Cx46, wild-type Hela cells ('H', lanes 13, 15, 17) or Hela cells stably transfected with Cx43 ('43'; lanes 14, 16, 18) were transiently transfected with Cx46 cDNA, then analyzed as described above for total Cx46 expression (lanes 13, 14), immunopurified Cx43 (lanes 15, 16) and coimmunopurified Cx46 (lanes 17, 18), except that anti-Cx43 was used for coimmunopurification. Consistent with the ability of Cx43 and Cx46 to form mixed oligomers, Cx46 was specifically coimmunopurified using Cx43 antibodies from Hela cells expressing both connexins (lane 16). (C-I) ROS cells ('R', lanes 19, 21) and type I-like alveolar epithelial cells, AEC ('A', lanes 20, 22) expressing endogenous Cx43 and Cx46 were also examined for the ability of Cx46 to coimmunopurify with anti-Cx43 IgG. By immunofluorescence, both cell types had Cx43 present at the plasma membrane (D,G); however, Cx46 showed differential localization to either TGN (E, arrows) or the plasma membrane (H, arrowheads), depending on cell phenotype. Bar, 10 μm. While comparable levels of Cx43 were immunopurified from both cell types using anti-Cx43 IgG (lanes 19, 20), Cx46 was only coimmunopurified with anti-Cx43 IgG from samples prepared from alveolar epithelial cells (lane 22).

present. However, since the voltage-gating properties of mixed Cx43/Cx56 gap junction channels are distinct from those of channels composed of Cx43 alone (Berthoud et al., 2000), this raises the possibility that unique gating characteristics of Cx43/Cx46 gap junction channels may be important for alveolar epithelial function.

Since Cx43 and Cx46 have the capacity to form mixed gap junction channels, cells which differentially sort Cx43 and Cx46 require an active mechanism or chaperone to prevent random connexin intermixing and heteromeric gap junction channel formation. The notion of connexin chaperones is also suggested by oligomerization occurring in post-ER compartments (Musil and Goodenough, 1993). One possibility is that cells which show differential localization of Cx43 and Cx46 also use differential targeting of these connexins to control whether they intermix. In support of this notion, multiple secretory pathways have been found to coexist in non-polarized cells (Chavez et al., 1996; Harsay and Bretscher, 1995; Yoshimori et al., 1996). Differential connexin targeting is also suggested by Guerrier et al. (Guerrier et al., 1995), who found that Cx32 was targeted to the apical plasma membrane while Cx43 was directed to the basolateral surface by polarized thyroid cells, although the innate incompatibility of Cx32 and Cx43 may also contribute to their differential sorting (see below). Identifying putative connexin-specific targeting motifs will enable the relationship between connexin targeting and sequence elements that regulate assembly and heteromeric channel formation to be determined.

By dendrogram analysis of primary amino acid sequence, connexins have been assigned to at least two major subfamilies, α and β (Kumar and Gilula, 1996). Since Cx43 and Cx46 are both α connexins, and Cx32 is a β connexin, our results are consistent with models where heteromeric gap junction assembly occurs only between connexins within the same subfamily (Yeager et al., 1998). For instance, Cx32 and Cx43 simultaneously translated in vitro do not form mixed gap junction hemichannels (Falk et al., 1997). In contrast, there are numerous examples where two different α connexins (Brink et al., 1997; Donaldson et al., 1995; Jiang and Goodenough, 1996; Koval et al., 1995) or two different β connexins intermix (Ahmad et al., 1999; Bevans et al., 1998; Stauffer, 1995). To date, gap junction channels containing both α and β connexins have not been isolated from cells or assembled in vitro. Whether all connexins within a subfamily are compatible to form heteromeric channels remains to be determined.

Cx43/β-gal as an inhibitor of gap junctional intercellular communication

This study confirmed that the dominant negative effect of Cx43/β-gal (Sullivan and Lo, 1995) is probably due to multiple mechanisms. First, Cx43/β-gal inhibits the transport of endogenous unmodified connexins to the cell surface, thus reducing the number of potential gap junction channels which can participate in intracellular communication. Second, Cx43/β-gal is also likely to interfere with gap junction channel activity or assembly at the plasma membrane, as inferred by the inhibition of Cx43 phosphorylation and decreased gap junction plaque size in the presence of Cx43/β-gal. Alterations in Cx43 phosphorylation may, in turn, affect the gating of these channels (Lampe et al., 2000; Paulson et al., 2000). Alternatively, the β-gal moiety may have a steric effect that directly blocks access to the channel.

The ability of Cx43/β-gal to inhibit the transport of both Cx43 and Cx46 in NIH 3T3 cells suggests that Cx43/β-gal has the capability to inhibit gap junctional communication mediated by multiple connexin isotypes. This may be particularly advantageous when analyzing the role of gap junctional communication in primary cells or in tissues of transgenic animals that are likely to express multiple endogenous connexins. The ability of Cx43/β-gal and other dominant negative connexin constructs to interact with multiple connexins underscores the utility of this approach as an alternative to studies with connexin-deficient mice for exploring physiological roles for gap junctions (Reume et al., 1995; Sullivan et al., 1998).

Cx43 assembly intermediates prior to the TGN

Previous biochemical analysis of Triton X-100 solubilized extracts from cells suggests that Cx43 hemichannel assembly occurs at the TGN (Koval et al., 1997; Musil and Goodenough, 1993). Using both sucrose gradient fractionation and chemical crosslinkers, Cx43 monomers and hexamers were the only detectable assembly intermediates. Musil and Goodenough used an extensive panel of inhibitors, including BFA, CCCP, 15°C temperature block and CHO cells with a temperature-sensitive block in transport to show that assembly of Cx43 into hexamers required transport to the TGN (Musil and Goodenough, 1993). In each case, they only detected monomeric Cx43 when transport to the TGN was inhibited. Monensin treatment also caused a three- to fourfold reduction in Cx43 oligomerization in ROS cells, again consistent with the TGN as the site for Cx43 hemichannel assembly (Koval et al., 1997). These data are most consistent with a model for Cx43 assembly where monomers are transported to the TGN, where they are then assembled into oligomeric complexes. Our results here are also consistent with this model for Cx43 assembly, since Cx43/β-gal inhibited Cx43 hexamer formation and the intracellular pool of Cx43 was largely in a perinuclear compartment prior to the TGN.

Since Cx43 and Cx43/β-gal interact prior to the site for Cx43 hemichannel assembly, the mechanism for dominant negative retention of Cx43 by Cx43/β-gal is not clear at present. Based on our results, though, we can rule out some possibilities. Given the molecular mass of the Cx43-Cx43/β-gal complex (Fig. 6B,C), it seems unlikely that interactions between β-galactosidase moieties are required, since this would be most likely to involve Cx43/β-gal tetramers (Jacobson et al., 1994) and little Cx43 comigrated with the heavy Cx43/β-gal fraction isolated from 43β cells. Also, an interaction due to Cx43/β-gal misfolding seems unlikely, since intracellular Cx43/β-gal was Triton X-100 soluble and was also found assembled into gap junctions at the plasma membrane (Fig. 4). One possibility is that the formation of a stable Cx43 + Cx43/β-gal intermediate may be enhanced by an increase in transit time for Cx43/β-gal containing intermediates through the Golgi apparatus, as has been observed for connexin fusion proteins containing an aequorin moiety (George et al., 1999). If this is the case, then the Cx43/β-gal protein may act as a trap to stabilize an intermediate that is otherwise highly transient and present at undetectable levels in unperturbed cells. Consistent with this, George et al. found that Cx43-aequorin and Cx32-aequorin chimeras transfected into COS-7 cells were assembled into sub-hexameric complexes as early as the ER and ERGIC (George et al., 1999) and also showed high levels of intracellular retention (George et al., 1998).

Interestingly, despite the assembly of some Cx43/β-gal into gap junctions in 43β2 cells, there was not a substantial Cx43 hexamer peak when the connexins were analyzed by sucrose gradient fractionation (Fig. 6C; region 3). Instead, most of the intracellular Cx43 was either monomeric or in subhexameric Cx43-Cx43/β-gal complexes. This suggests that disruption of Cx43 trafficking by Cx43/β-gal expression depletes the TGN pool of hexameric Cx43 and implies that exit from the TGN is the normal rate-limiting step in transport of oligomerized Cx43 to the cell surface.

It is tempting to speculate that Cx43-Cx43/β-gal complexes accumulating in the pre-TGN compartment of 43β2 cells reflect a *bona fide* intermediate in the Cx43 assembly pathway. Cx43/β-gal behaves in a manner analogous to endogenous Cx43 in that (1) it interacts specifically with unmodified Cx43 and Cx46, but not Cx32, (2) the intracellular pool of Cx43/β-gal is largely soluble under conditions where Cx43 is soluble, (3) Cx43/β-gal localized to gap junctions is largely insoluble under conditions where Cx43 is insoluble and (4) cells expressing low levels of Cx43/β-gal show Cx43/β-gal at the cell surface (Fig. 2) and also decreased gap junctional communication (Sullivan and Lo, 1995), consistent with assembly of Cx43/β-gal into gap junction channels. However, since the mechanism for Cx43/β-gal retention in a pre-TGN compartment remains undefined, we cannot be certain that Cx43-Cx43/β-gal complexes reflect an assembly intermediate. A likely alternative is that the intracellular pool of Cx43-Cx43/β-gal complexes may be an intermediate in transit to a degradation quality control pathway (VanSlyke et al., 2000), since we cannot rule out the possibility that these pre-TGN connexin complexes were induced by Cx43/β-gal. Nonetheless, putative stable subhexameric Cx43 complexes would likely be highly transient and unstable intermediates in connexin oligomerization, since native subhexameric connexin intermediates have not been successfully isolated to date. Also, it seems plausible that putative Cx43 assembly intermediates may require cofactors that are not stable under the solubilization conditions currently used to analyze connexin assembly. If this is the case, then further analysis of Cx43 assembly will benefit from the use of constructs containing specific retention motifs for targeting to specific intracellular compartments, such as the ER or ERGIC, which will enable the trapping of assembly intermediates in intact cells.

We are extremely grateful to Dr R. Sullivan for the preparation of the stably transfected 3T3 cell lines used in this study. We thank Drs M. Beers and C. Deutsch for critical reading of the manuscript. Also, we thank Dr N. Gonatas for the generous gift of anti-MG160 antiserum and Dr S. Scherer for providing the Cx32 construct. This work was supported by a Hulda Irene Duggan Investigator Award of the Arthritis Foundation, an American Heart Association Grant in Aid and NIH GM61012 to M.K., and NIH HD36457 and NSF IBN-31544 to C.W.L.

REFERENCES

Abraham, V., Chou, M. L., DeBolt, K. M. and Koval, M. (1999). Phenotypic control of gap junctional communication by cultured alveolar epithelial cells. *Am. J. Physiol.* **276**, L825-834.

Abraham, V., Chou, M. L., George, P., Pooler, P., Zaman, A., Savani, R. C. and Koval, M. (2001). Heterocellular gap junctional communication between alveolar epithelial cells. *Am. J. Physiol. Lung Cell Mol. Physiol.* **280**, L1085-1093.

Ahmad, S., Diez, J. A., George, C. H. and Evans, W. H. (1999). Synthesis and assembly of connexins in vitro into homomeric and heteromeric functional gap junction hemichannels. *Biochem. J.* **339**, 247-253.

Berthoud, V. M., Montegna, E. A., Atal, N., Aithal, N. H., Brink, P. R. and Beyer, E. C. (2000). Heteromeric connexons formed by the lens connexins, connexin43 and connexin56. *Eur. J. Cell Biol.* **80**, 11-19.

Bevans, C. G., Kordel, M., Rhee, S. K. and Harris, A. L. (1998). Isoform composition of connexin channels determines selectivity among second messengers and uncharged molecules. *J. Biol. Chem.* **273**, 2808-2816.

Brink, P. R., Cronin, K., Banach, K., Peterson, E., Westphale, E. M., Seul, K. H., Ramanan, S. V. and Beyer, E. C. (1997). Evidence for heteromeric gap junction channels formed from rat connexin43 and human connexin37. *Am. J. Physiol.* **273**, C1386-1396.

Chavez, R. A., Miller, S. G. and Moore, H. P. (1996). A biosynthetic regulated secretory pathway in constitutive secretory cells. *J. Cell Biol.* **133**, 1177-1191.

Civitelli, R., Beyer, E. C., Warlow, P. M., Robertson, A. J., Geist, S. T. and Steinberg, T. H. (1993). Connexin43 mediates direct intercellular communication in human osteoblastic cell networks. *J. Clin. Invest.* **91**, 1888-1896.

Cruciani, V. and Mikalsen, S. O. (1999). Stimulated phosphorylation of intracellular connexin43. *Exp. Cell Res.* **251**, 285-298.

Dobbs, L. G., Gonzalez, R. and Williams, M. C. (1986). An improved method for isolating type II cells in high yield and purity. *Am. Rev. Respir. Dis.* **134**, 141-145.

Donaldson, P. J., Dong, Y., Roos, M., Green, C., Goodenough, D. A. and Kistler, J. (1995). Changes in lens connexin expression lead to increased gap junctional voltage dependence and conductance. *Am. J. Physiol.* **269**, C590-600.

Falk, M. M., Buehler, L. K., Kumar, N. M. and Gilula, N. B. (1997). Cell-free synthesis and assembly of connexins into functional gap junction membrane channels. *EMBO J.* **16**, 2703-2716.

Garcia-Mata, R., Bebok, Z., Sorscher, E. J. and Sztul, E. S. (1999). Characterization and dynamics of aggresome formation by a cytosolic GFP-chimera. *J. Cell Biol.* **146**, 1239-1254.

George, C. H., Kendall, J. M., Campbell, A. K. and Evans, W. H. (1998). Connexin-aequorin chimerae report cytoplasmic calcium environments along trafficking pathways leading to gap junction biogenesis in living COS-7 cells. *J. Biol. Chem.* **273**, 29822-29829.

George, C. H., Kendall, J. M. and Evans, W. H. (1999). Intracellular trafficking pathways in the assembly of connexins into gap junctions. *J. Biol. Chem.* **274**, 8678-8685.

Goliger, J. A., Bruzzone, R., White, T. W. and Paul, D. L. (1996). Dominant inhibition of intercellular communication by two chimeric connexins. *Clin. Exp. Pharmacol. Physiol.* **23**, 1062-1067.

Gonatas, J. O., Mezitis, S. G., Stieber, A., Fleischer, B. and Gonatas, N. K. (1989). MG-160. A novel sialoglycoprotein of the medial cisternae of the Golgi apparatus. *J. Biol. Chem.* **264**, 646-653.

Goodenough, D. A., Goliger, J. A. and Paul, D. L. (1996). Connexins, connexons and intercellular communication. *Ann. Rev. Biochem.* **65**, 475-502.

Guerrier, A., Fonlupt, P., Morand, I., Rabilloud, R., Audebet, C., Krutovskikh, V., Gros, D., Rousset, B. and Munari-Silem, Y. (1995). Gap junctions and cell polarity: connexin32 and connexin43 expressed in polarized thyroid epithelial cells assemble into separate gap junctions, which are located in distinct regions of the lateral plasma membrane domain. *J. Cell Sci.* **108**, 2609-2617.

Harsay, E. and Bretscher, A. (1995). Parallel secretory pathways to the cell surface in yeast. *J. Cell Biol.* **131**, 297-310.

Jacobson, R. H., Zhang, X. J., DuBose, R. F. and Matthews, B. W. (1994). Three-dimensional structure of beta-galactosidase from *E. coli*. *Nature* **369**, 761-766.

Jiang, J. X. and Goodenough, D. A. (1996). Heteromeric connexons in lens gap junction channels. *Proc. Natl. Acad. Sci. USA* **93**, 1287-1291.

Jiang, J. X., Paul, D. L. and Goodenough, D. A. (1993). Posttranslational phosphorylation of lens fiber connexin46: a slow occurrence. *Invest. Ophthalmol. Visual Sci.* **34**, 3558-3565.

Johnston, J. A., Ward, C. L. and Kopito, R. R. (1998). Aggresomes: a cellular response to misfolded proteins. *J. Cell Biol.* **143**, 1883-1898.

Kelsell, D. P., Dunlop, J. and Hodgins, M. B. (2001). Human diseases: clues to cracking the connexin code? *Trends Cell Biol.* **11**, 2-6.

Konig, N. and Zampighi, G. A. (1995). Purification of bovine lens cell-to-cell channels composed of Connexin44 and Connexin50. *J. Cell Sci.* **108**, 3091-3098.

Koval, M., Geist, S. T., Westphale, E. M., Kemendy, A. E., Civitelli, R., Beyer, E. C. and Steinberg, T. H. (1995). Transfected connexin45 alters gap junction permeability in cells expressing endogenous connexin43. *J. Cell Biol.* **130**, 987-995.

Koval, M., Harley, J. E., Hick, E. and Steinberg, T. H. (1997). Connexin46 is retained as monomers in a trans-Golgi compartment of osteoblastic cells. *J. Cell Biol.* **137**, 847-857.

Krutovskikh, V. A., Yamasaki, H., Tsuda, H. and Asamoto, M. (1998). Inhibition of intrinsic gap-junction intercellular communication and enhancement of tumorigenicity of the rat bladder carcinoma cell line BC31 by a dominant-negative connexin 43 mutant. *Mol. Carcinog.* **23**, 254-261.

Kumar, N. M., Friend, D. S. and Gilula, N. B. (1995). Synthesis and assembly of human beta(1) gap junctions in BHK cells by DNA transfection with the human beta(1) cDNA. *J. Cell Sci.* **108**, 3725-3734.

Kumar, N. M. and Gilula, N. B. (1996). The gap junction communication channel. *Cell* **84**, 381-388.

Laird, D. W., Castillo, M. and Kasprzak, L. (1995). Gap junction turnover, intracellular trafficking, and phosphorylation of connexin43 in brefeldin A-treated rat mammary tumor cells. *J. Cell Biol.* **131**, 1193-1203.

Lampe, P. D., Kurata, W. E., Warn-Cramer, B. J. and Lau, A. F. (1998). Formation of a distinct connexin43 phosphoisoform in mitotic cells is dependent upon p34cdc2 kinase. *J. Cell Sci.* **111**, 833-841.

Lampe, P. D., TenBroek, E. M., Burt, J. M., Kurata, W. E., Johnson, R. G. and Lau, A. F. (2000). Phosphorylation of connexin43 on serine368 by protein kinase C regulates gap junctional communication. *J. Cell Biol.* **149**, 1503-1512.

Lippincott-Schwartz, J., Yuan, L., Tipper, C., Amherdt, M., Orci, L. and Klausner, R. D. (1991). Brefeldin A's effects on endosomes, lysosomes, and the TGN suggest a general mechanism for regulating organelle structure and membrane traffic. *Cell* **67**, 601-616.

Lippincott-Schwartz, J., Yuan, L. C., Bonifacino, J. S. and Klausner, R. D. (1989). Rapid redistribution of Golgi proteins into the ER in cells treated with brefeldin A: evidence for membrane cycling from Golgi to ER. *Cell* **56**, 801-813.

Musil, L. S., Cunningham, B. A., Edelman, G. M. and Goodenough, D. A. (1990). Differential phosphorylation of the gap junction protein connexin43 in junctional communication-competent and -deficient cell lines. *J. Cell Biol.* **111**, 2077-2088.

Musil, L. S. and Goodenough, D. A. (1991). Biochemical analysis of connexin43 intracellular transport, phosphorylation, and assembly into gap junctional plaques. *J. Cell Biol.* **115**, 1357-1374.

Musil, L. S. and Goodenough, D. A. (1993). Multisubunit assembly of an integral plasma membrane channel protein, gap junction connexin43, occurs after exit from the ER. *Cell* **74**, 1065-1077.

Pagano, R. E., Sepanski, M. A. and Martin, O. C. (1989). Molecular trapping of a fluorescent ceramide analogue at the Golgi apparatus of fixed cells: interaction with endogenous lipids provides a trans-Golgi marker for both light and electron microscopy. *J. Cell Biol.* **109**, 2067-2079.

Paul, D. L., Yu, K., Bruzzone, R., Gimlich, R. L. and Goodenough, D. A. (1995). Expression of a dominant negative inhibitor of intercellular communication in the early Xenopus embryo causes delamination and extrusion of cells. *Development* **121**, 371-381.

Paulson, A. F., Lampe, P. D., Meyer, R. A., TenBroek, E., Atkinson, M. M., Walseth, T. F. and Johnson, R. G. (2000). Cyclic AMP and LDL trigger a rapid enhancement in gap junction assembly through a stimulation of connexin trafficking. *J. Cell Sci.* **113**, 3037-3049.

Reaves, B. and Banting, G. (1992). Perturbation of the morphology of the trans-Golgi network following Brefeldin A treatment: redistribution of a TGN-specific integral membrane protein, TGN38. *J. Cell Biol.* **116**, 85-94.

Reume, A. G., deSousa, P. A., Kulkarni, S., Langille, B. L., Zhu, D., Davies, T. C., Juneja, S. C., Kidder, G. M. and Rossant, J. (1995). Cardiac malformation in neonatal mice lacking connexin43. *Science* **267**, 1831-1834.

Scherer, S. S., Deschenes, S. M., Xu, Y. T., Grinspan, J. B., Fischbeck, K. H. and Paul, D. L. (1995). Connexin32 is a myelin-related protein in the PNS and CNS. *J. Neurosci.* **15**, 8281-8294.

Simon, A. M. and Goodenough, D. A. (1998). Diverse functions of vertebrate gap junctions. *Trends Cell Biol.* **8**, 477-483.

Stauffer, K. A. (1995). The gap junction proteins β1-connexin (connexin32) and β2-connexin (connexin26) can form heteromeric hemichannels. *J. Biol. Chem.* **270**, 6768-6772.

Sullivan, R., Huang, G. Y., Meyer, R. A., Wessels, A., Linask, K. K. and Lo, C. W. (1998). Heart malformations in transgenic mice exhibiting dominant negative inhibition of gap junctional communication in neural crest cells. *Dev. Biol.* **204**, 224-234.

Sullivan, R. and Lo, C. W. (1995). Expression of a connexin 43/beta-galactosidase fusion protein inhibits gap junctional communication in NIH3T3 cells. *J. Cell Biol.* **130**, 419-429.

VanSlyke, J. K., Deschenes, S. M. and Musil, L. S. (2000). Intracellular transport, assembly, and degradation of wild-type and disease-linked mutant gap junction proteins. *Mol. Biol. Cell* **11**, 1933-1946.

Yeager, M., Unger, V. M. and Falk, M. M. (1998). Synthesis, assembly and structure of gap junction intercellular channels. *Curr. Opin. Struct. Biol.* **8**, 517-524.

Yoshimori, T., Keller, P., Roth, M. G. and Simons, K. (1996). Different biosynthetic transport routes to the plasma membrane in BHK and CHO cells. *J. Cell Biol.* **133**, 247-256.